

Collision induced migration of adsorbates on surfaces

L. Romm and M. Asscher

*Department of Physical Chemistry and Farkas Center for Light Induced Processes,
The Hebrew University, Jerusalem, 91904, Israel*

Y. Zeiri

Department of Chemistry, Nuclear Research Center, Negev, P.O.B. 9001, Beer-Sheva, Israel

(Received 11 January 1999; accepted 17 March 1999)

Collision induced migration (CIM) has been identified as a new surface phenomenon and has been studied for the first time using molecular dynamics simulations. The CIM process was represented by an energetic gas phase argon atom, striking an adsorbed nitrogen molecule on Ru(001). The efficiency of CIM was investigated as a function of the collider initial kinetic energy and angle of incidence. It was found that at low coverages an adsorbed molecule can migrate more than 150 Å following collisions at high energies and grazing angles of incidence. As coverage increases, inter-adsorbate collisions result in significant reduction of migration distances. At high energies, the competing process of collision induced desorption becomes dominant, leaving behind molecules which migrate shorter distances. These competing channels lead to a collision energy for which CIM is maximized. For the N₂/Ru system, the CIM process is most effective near collider energy of 2.0 eV. This new surface phenomenon of CIM has to be considered for better understanding the full range of surface processes which govern industrial high pressure catalysis. At the tail of the thermal kinetic energy distribution, energetic colliders from the gas phase lead to CIM and generate high energy inter-adsorbate collisions, sometimes discussed in terms of "hot-particle" chemistry.

© 1999 American Institute of Physics. [S0021-9606(99)70322-3]

I. INTRODUCTION

Diffusion of adsorbates on solid surfaces is of major importance for understanding the kinetics of heterogeneous catalytic reactions. It is well established that surface diffusion of atomic and molecular adsorbates on metal surfaces precedes desorption and starts at lower surface temperatures.¹ This is due to the fact that on metal surfaces the barrier for surface diffusion (E_{diff}) is smaller than the activation energy for desorption (E_{des}), typically $E_{\text{diff}} \approx (0.2 \pm 0.1)E_{\text{des}}$. Experimental information on barriers for surface diffusion of atoms and molecules have been rapidly accumulated in recent years, both on macroscopic diffusion lengths and on the microscopic scale. The macroscopic range provides information on the so-called chemical diffusion constant,¹ employing laser based techniques,²⁻⁸ while the microscopic view on the tracer diffusion coefficient¹ has been traditionally studied using high field techniques⁹⁻¹¹ and recently by STM.¹²⁻¹⁴

The effect of energetic colliders on surface processes such as desorption (CID)¹⁵⁻²⁰ and reaction (CIR)^{21,22} have been demonstrated. These processes were considered as possible new routes for surface reactivity in industrial catalysis, where energetic gas phase molecules in the tail of the Boltzmann distribution can affect the heterogeneous catalytic processes.^{15,16}

With this background of collision induced surface processes that have already been investigated, it is rather surprising to realize that the far more probable collision induced migration (CIM) has never been considered, neither theoretically nor experimentally.

The purpose of this study is to demonstrate the efficiency of CIM and the distances that adsorbates can migrate along the surface following energetic collisions at surface temperatures for which no thermal diffusion is expected. Moreover, it is anticipated that inter-adsorbate collisions can occur with sufficient relative energy to overcome activation barriers for surface reactions which at thermal energies are impossible to surmount. This should open new surface reactive channels.

The results reported here are based on classical molecular dynamics simulations. They correspond to the CIM of adsorbed nitrogen molecules on Ru(001) at 90 K following collisions with gas phase argon atoms. The complimentary study of collision induced desorption of N₂ from Ru(001) has very recently been investigated both experimentally and theoretically.^{20,23}

II. RESULTS AND DISCUSSION

The details of the MD simulations and the interaction potentials employed have been described elsewhere.^{20,23} Briefly, the Ru(001) single crystal is described by a slab of two moveable layers. In addition, there are two layers of fixed particles and a layer of fictitious particles attached to the bottom layer of the moving Ru atoms. The validity of this approach to correctly account for energy dissipation has been discussed in the literature.^{15,24} Each moveable layer consists of $7 \times 8 = 56$ atoms. Periodic boundary conditions are imposed in the X and Y directions. Adsorbate molecules are placed in the three-fold hollow sites with the molecular axis oriented normal to the surface plane. The minimum

adsorbate-adsorbate separation is set to be equal to $2.669 \times \sqrt{3} = 4.62 \text{ \AA}$, where 2.669 \AA is the lattice parameter of the hexagonal Ru(001). The motion of ruthenium atoms is governed by harmonic forces, with the surface temperature set constant at 90 K. Adsorbate-surface interaction has the form of a sum of pairwise Morse potentials, where the distance is set between i th Ru atom and the molecular center of mass. The interaction between the Ar collider and the surface atoms is described by a truncated pairwise Morse form, the interaction between the collider atom and the adsorbate is presented by a sum of Lennard-Jones potentials between the projectile and each nitrogen atom. Repulsive interaction among the adsorbates at higher coverages is represented by a sum of pairwise exponential terms describing the interaction between nitrogen atoms that belong to different molecules. The adsorbate intramolecular potential is described by a Morse function. The details of all the parameters for these potentials and interactions have been described in Ref. 23.

The target adsorbate (TM) is the molecule directly bombarded by the collider. In all the simulations the TM was chosen as the adsorbate positioned at the shortest distance from the slab. All other dynamic parameters of the collision were explained in detail in the previous publications.^{20,23} The integration time step is equal to 1 fs and the full integration time for an individual trajectory was limited to 10 ps throughout this study. The trajectory terminates upon completion of one of the following two conditions: either the molecule(s) desorb or maximum integration time has been reached.

Here we present the results of the first attempt to study collision induced migration. Molecular dynamics simulations enable us to examine the energy, angular, and coverage dependence of the average adsorbate migration distance, following the collision. We have also investigated the migration of neighbor molecules at higher coverages, but found that these molecules are only slightly displaced from their initial position as a result of collision with the recoiling TM. The following initial conditions for the collider were employed: Kinetic energy of $E_{\text{in}} = 0.4, 0.8, 1.45, 2.25,$ and 4.0 eV ; Angle of incidence (with respect to the surface normal) $\theta_{\text{in}} = 0^\circ, 40^\circ, 60^\circ$; Coverage $\Theta = 0.018$ (1 molecule on the slab); 0.036 (2 molecules); 0.072 (4 molecules); 0.125 (7 molecules), and 0.21 (12 molecules). For any given combination of these parameters, 3000 trajectories were calculated to obtain satisfactory statistics. For incident energies above a threshold value of 0.5 eV , CID gradually becomes a competing channel, as was shown before.^{20,23} It should be noted that for all parameter values examined we did not find evidence for vibrational excitation of the adsorbate. The interaction with the collider lead only to energy transfer to the translational and rotational modes of the N_2 .

In Fig. 1(a)–(c) the average migration distance of the target molecule (TM) is shown for increasing impact parameters at $E_{\text{in}} = 1.45 \text{ eV}$, $\theta_{\text{in}} = 0^\circ, 40^\circ, 60^\circ$, for the indicated initial coverages. The average migration distance (AMD) is defined as the distance between the position of the TM at $t = 0$ and after 10 ps, averaged over the impact parameters within a given range, for all nondesorbing trajectories. It is clearly seen that at normal incidence maximum displacement

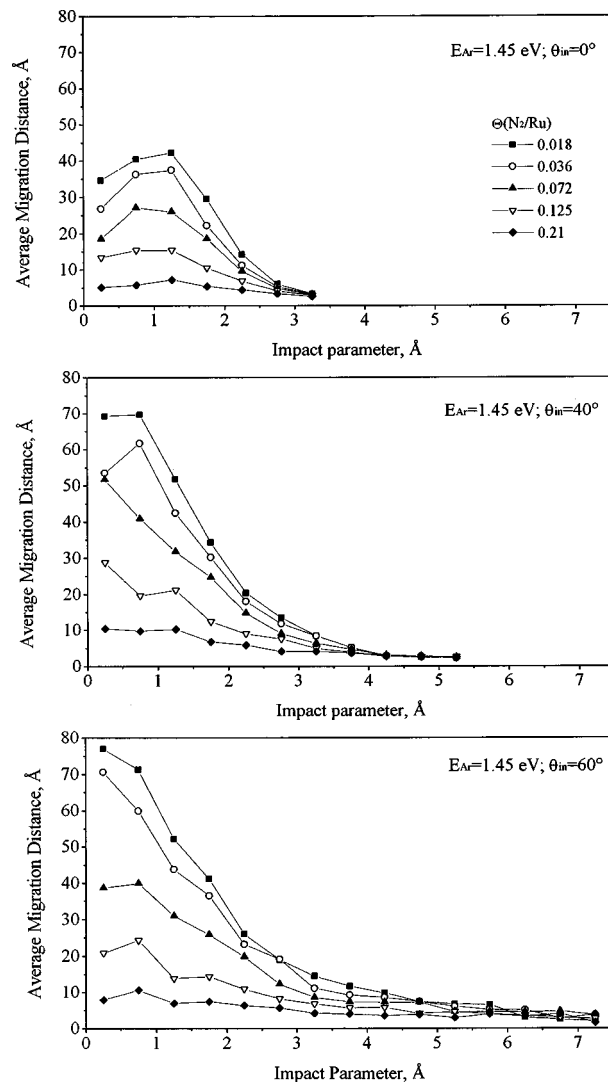


FIG. 1. Average migration distance (AMD) of the target nitrogen molecule (TM) as a function of the impact parameter for the collision. The incidence energy is 1.45 eV and the angles of incidence are $\theta_{\text{in}} = 0^\circ, 40^\circ,$ and 60° . The average number of trajectories for each point is 20–70 for impact parameters up to 1.5 \AA and it grows to 120–150 for the impact parameter range 1.5 – 2.5 \AA and up to 300 for higher impact parameters.

of the TM is reached at nonzero impact parameter ($b_{\text{imp}} \approx 1 \text{ \AA}$). At this collision geometry the energy transferred from the collider to the adsorbate is channeled most effectively into lateral migration of the adsorbate. At off-normal angles of incidence (40° and 60°), trajectories having $b_{\text{imp}} \approx 0 \text{ \AA}$ are the most effective to induce long migration distances. A strong dependence of AMD on θ_{in} is observed. The migration distances shown in Fig. 1 reflect the remarkable efficiency of the CIM process.

As coverage increases the AMD significantly shortens, while the CIM process attenuates. This is a direct consequence of the multiple inter-adsorbates collisions between the TM and its neighbor adsorbates, which block the original direction of motion of the TM on the surface. For all these angles of incidence, the AMD decreases by nearly an order of magnitude when the coverage increases from 1 ($\Theta = 0.018$) to 12 ($\Theta = 0.21$) molecules on the slab.

In Fig. 2 the effect of the incidence kinetic energy of the

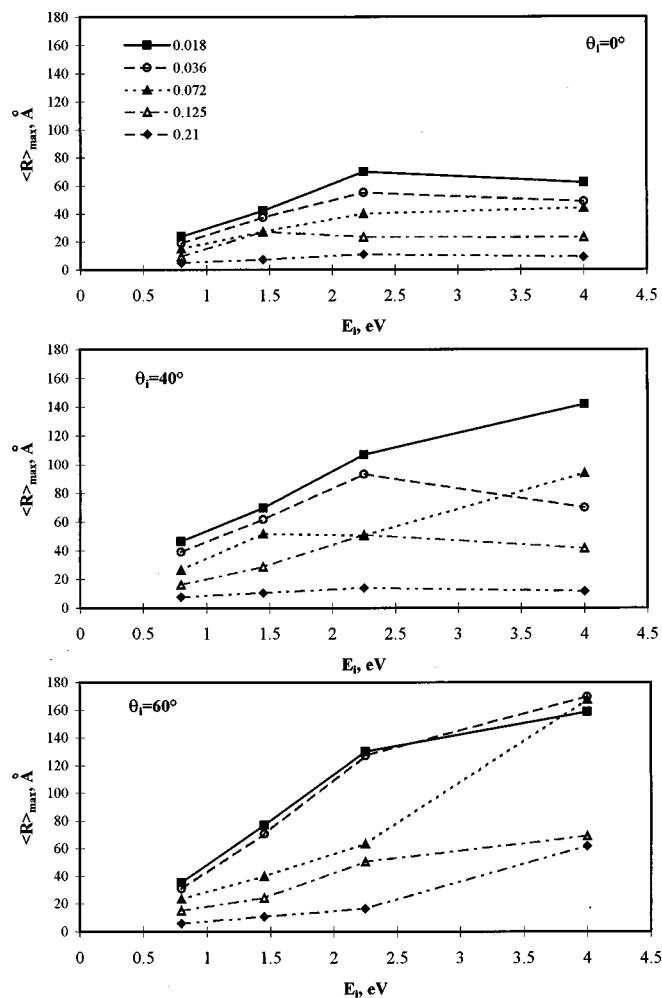


FIG. 2. Average maximum migration distance $\langle R_{\max} \rangle$ as a function of the Ar collision energy for different coverages and three angles of incidence $\theta_{in} = 0^\circ$, 40° , and 60° , as indicated.

Ar atoms is shown for three angles of incidence and different coverages. Instead of the AMD, as described above, this figure displays a number which we call the maximum migration distance— R_{\max} —and is defined as the longest distance obtained at the most effective impact parameter range. The numbers obtained this way are used in order to emphasize the variation in the efficiency of the CIM process with the various collision parameters and coverage. As expected the migration distance increases with the collider's energy and can reach more than 150 \AA at angle of incidence of 60° at the lowest coverages. It is interesting to note, however, that above 2.2 eV R_{\max} decreases for $\theta_{in} = 0^\circ$ and 40° . In addition, it has been found that at the highest coverage, the CIM distance practically does not change as the projectile energy increases due to the efficient quenching of the initial kinetic energy of the TM by inter-adsorbates collisions. It is somewhat different at 60° , where an increase of R_{\max} is observed even at the highest coverage above 2.5 eV .

The tendency for decreasing R_{\max} at collision energies above 2.2 eV can be explained by the competing collision induced desorption which becomes the dominant process. The CID events necessarily include the more energetic trajectories. As a result, the trajectories which represent the

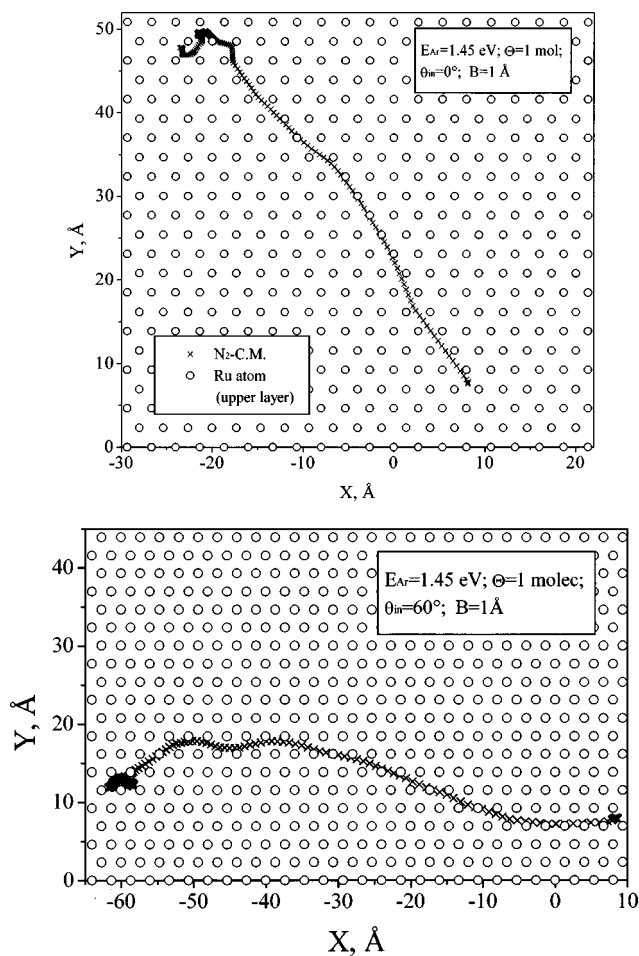


FIG. 3. Typical trajectories following collision induced migration at the indicated parameters.

molecules left on the surface are those with the lower kinetic energy in the tail of the distribution obtained following collisions with the energetic rare gas. The balance between these competing events, therefore, results in a maximum R_{\max} which is observed near 2.0 eV . The longest migration distance shifts to higher energies for increasing angles of incidence, as seen in the case of $\theta_{in} = 60^\circ$. This is due to the fact that both the CID and CIM processes become more efficient at larger θ_{in} , but CIM grows faster. This conclusion is clearly seen at higher coverages, where the inter-adsorbate collisions reduce more effectively the probability for CID than for CIM.

Better understanding of the CIM dynamics is gained by the examination of individual trajectories. Figure 3 presents typical migration trajectory obtained following collision of Ar at $E_{in} = 1.45 \text{ eV}$; $\Theta = 0.018$ (1 molecule on the slab); $b_{imp} = 1 \text{ \AA}$ for normal angle of incidence $\theta_{in} = 0^\circ$. This trajectory reveals a “classical” billiard ball motion along an initial impact direction for quite a long distance. The kinetic energy is high enough to enable this motion regardless of the energy barriers experienced by the adsorbate during its migration. Inspection of the vertical position of the adsorbate center of mass during its migration process, shown in Fig. 4, reveals that during the first 2–5 ps following the collision, the molecules reside about $0.3\text{--}0.5 \text{ \AA}$ above their equilib-

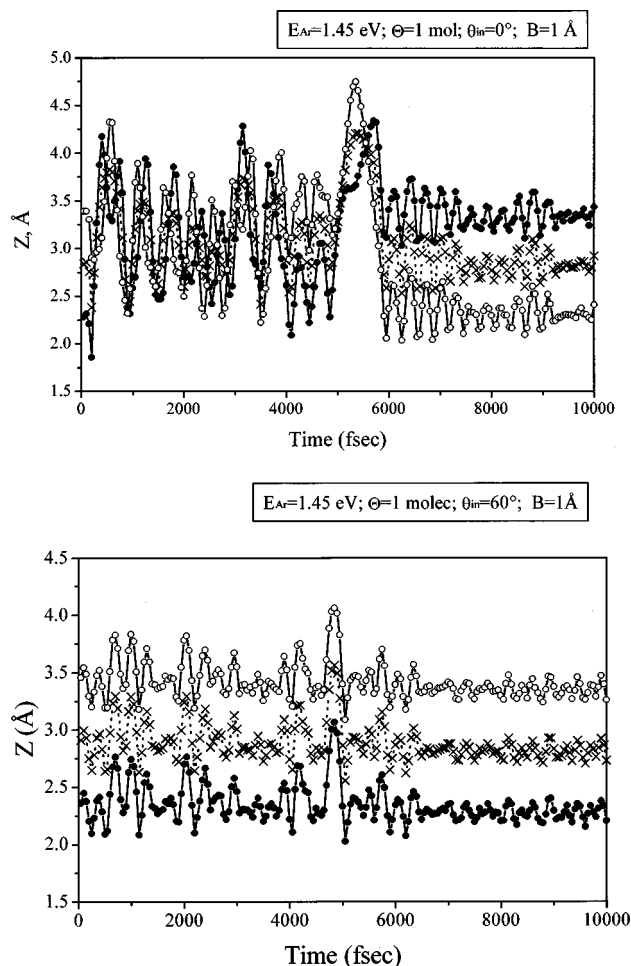


FIG. 4. The Z direction coordinates of each of the nitrogen atoms in the adsorbed N_2 molecule (open and filled circles) and the center of mass (\times) of the TM as a function of time following the CIM event. The coordinates correspond to the two trajectories shown in Fig. 3.

rium position (which is 2.8 \AA). This dramatic elevation in the adsorbate normal position results in a nearly free migration, practically without any barrier for surface diffusion. For example, during this time the barrier for migration over the on-top sites decreases from 0.25 to 0.03 eV . Over the other sites there is practically no barrier for diffusion even at the equilibrium normal distance of 2.8 \AA . At grazing collisions the high tangential energy can cause long migrations without the need for such dramatic center of mass elevation, as seen in Fig. 4.

Approaching the end of its migration, the TM has lost most of its tangential kinetic energy to the surface and neighbor adsorbates at high coverages. At this stage it can only hop a few more times between neighbor adsorption sites before it relaxes into its final position. At normal angle of incidence during the initial $2\text{--}5 \text{ ps}$, the admolecule experiences a complicated trajectory composed of rotation and sliding along the surface, as seen in Fig. 4. This is possibly another reason for the shorter migration distance observed at this incidence angle. In this case some fraction of the available energy is transferred to the rotational-tumbling motion.

We have also examined the individual trajectories of incidence energy below the threshold for CID, $E_{in} = 0.4 \text{ eV}$. At

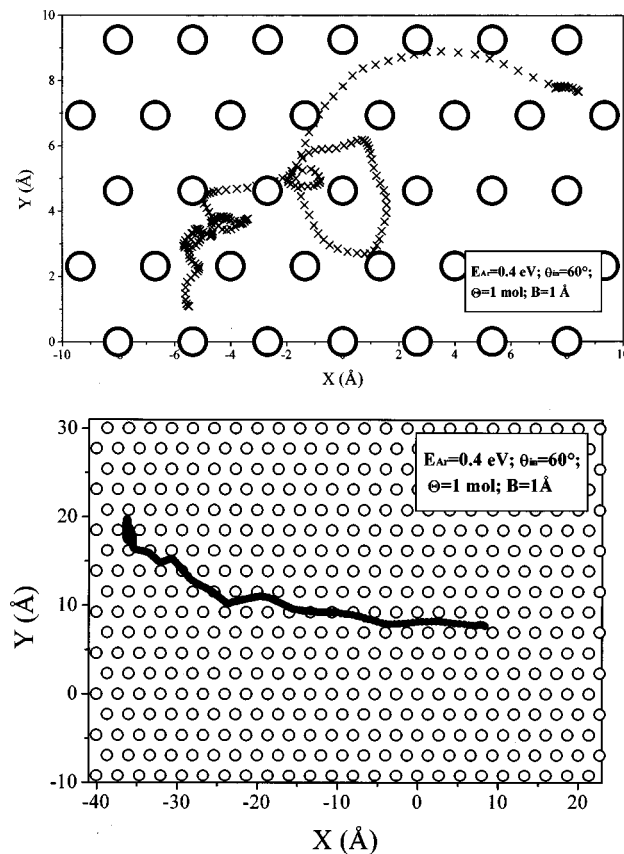


FIG. 5. Typical trajectories for collisions at energy of 0.4 eV which is below the threshold for desorption at the indicated parameters.

this energy one finds rather long CIM distances at low coverages, up to 40 \AA . However, many trajectories show complicated migration paths due to their low kinetic energy and the highly corrugated PES. Some typical trajectories are shown in Fig. 5.

The effect of neighbor adsorbates on the direction of motion of the TM has been examined as well. It was observed that in most cases the TM is the only admolecule which actually migrates, while its neighbors only slightly move from their initial position. In a small number of cases, in particular for large angles of incidence, we could also observe the classical ‘‘billiard ball’’ motion, where the TM is blocked by a neighbor adsorbate which in turn travels up to 20 \AA away from its original position. Typical trajectories at high coverage are shown in Fig. 6.

Finally, in order to estimate how the CIM process can be followed experimentally, one has to integrate the AMD values (IAMD) shown in Fig. 1 over the entire impact parameter range. The values of IAMD obtained this way were then calculated for different coverages as a function of Ar kinetic energy. The results are shown in Fig. 7 for two angles of incidence, $\Theta_{in} = 0^\circ$ and 60° . It is clear that the integrated average migration distance is about a factor of 5 shorter. Moreover, the energy dependence is also far more modest than that obtained for R_{max} ; see Fig. 2. The reason for this effect is that there are many more Ar trajectories at large impact parameters which result in small AMD (see Fig. 1) than those with small impact parameters and large AMD. As

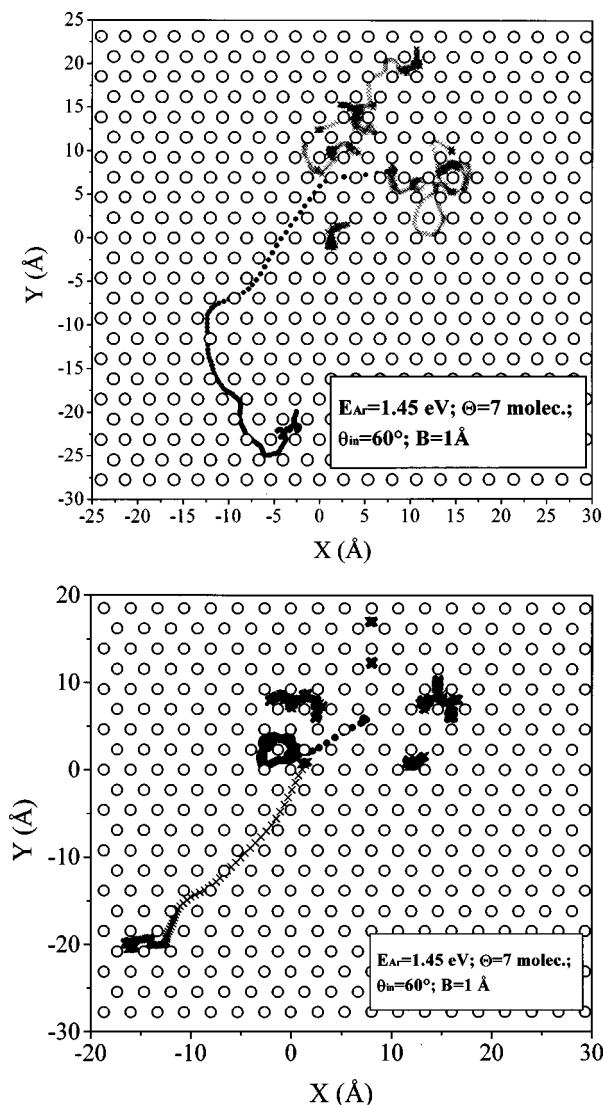


FIG. 6. Typical trajectories for collisions at incidence energy of 1.45 eV, $\theta_{in}=60^\circ$ at high coverage (7 molecules, $\Theta=0.125$).

the collision energy increases, the AMD values at small impact parameters increase, but at the same time the number of trajectories at large impact parameters also increase. The result is a compensation which diminishes the overall efficiency and energy dependence of the CIM process.

III. CONCLUSIONS

A new surface phenomenon has been identified and discussed for the first time. It involves the surface migration of an adsorbate, induced by collision between an energetic gas particle and an adsorbate—collision induced migration. The CIM process has been studied using molecular dynamics simulations of the Ar/N₂/Ru(001) system. It was found that single adsorbed molecule can migrate over 150 Å following collisions at high energies and large angles of incidence. As coverage increases, inter-adsorbate collisions efficiently quench the migration distance. At high energies, the competing collision induced desorption becomes dominant, leaving behind only low energy adsorbates which migrate to relatively short distances. This results in an optimum collision

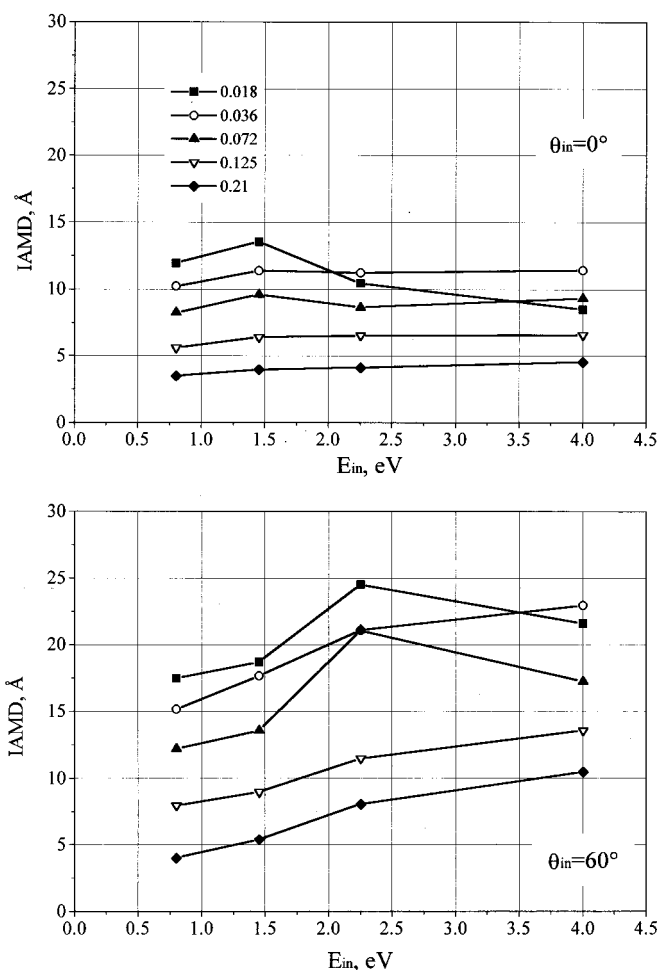


FIG. 7. The integral average migration distance (IAMD) as a function of the Ar collision energy for the indicated coverages and angles of incidence.

energy for the most efficient CIM process near 2.0 eV. It was observed that the target molecule migrates for long distances due to the fact that its center of mass is found to reside more than 0.5 Å above its equilibrium adsorption position for 2–5 ps, during which it has a very small barrier for diffusion. An interesting open question which arises from this study and needs to be addressed in the future is the conceptual similarity and difference between CIM and thermal diffusion.

The study of a new surface phenomenon—collision induced migration—should affect our interpretation and understanding of industrial high pressure catalytic processes. At the tail of the thermal kinetic energy distribution, energetic colliders from the gas phase lead to CIM and generate high energy inter-adsorbate collisions, sometimes discussed in terms of ‘‘hot-particle’’ chemistry. The CIM can also induce efficient mixing of adsorbed phases and thus enhance surface reactions.

ACKNOWLEDGMENTS

This work has been partially supported by a grant from the Israel Science Foundation and by the German Israel Foundation. The Farkas Center for Light Induced Processes

is supported by the Bundesministerium für Forschung und Technologie and the Minerva Gesellschaft für die Forschung mbH.

- ¹G. Ehrlich and K. J. Stolt, *Annu. Rev. Phys. Chem.* **31**, 603 (1980); R. Gomer, *Rep. Prog. Phys.* **53**, 917 (1990).
- ²C. H. Mak, B. G. Koehler, J. L. Brand, and S. M. George, *J. Chem. Phys.* **87**, 2340 (1987).
- ³D. E. Brown, D. S. Sholl, R. T. Skodje, and S. M. George, *Chem. Phys.* **201**, 273 (1995).
- ⁴X. D. Zhu, Th. Raising, and Y. R. Shen, *Phys. Rev. Lett.* **61**, 2883 (1988).
- ⁵G. A. Reider, U. Höfer, and T. F. Heinz, *Phys. Rev. Lett.* **66**, 1994 (1991).
- ⁶X. D. Zhu, A. Lee, A. Wong, and U. Linke, *Phys. Rev. Lett.* **68**, 1862 (1992).
- ⁷Z. Rosenzweig, I. Farbman, and M. Asscher, *J. Chem. Phys.* **98**, 8277 (1993).
- ⁸W. Zhao, R. W. Verhoef, and M. Asscher, *J. Chem. Phys.* **107**, 5554 (1997).
- ⁹G. Mazenko, J. R. Banavar, and R. Gomer, *Surf. Sci.* **107**, 459 (1981).
- ¹⁰Y. Song and R. Gomer, *Surf. Sci.* **295**, 174 (1993).
- ¹¹S. C. Wang and G. Ehrlich, *Phys. Rev. Lett.* **70**, 41 (1993); D. C. Senft and G. Ehrlich, *ibid.* **74**, 294 (1995).
- ¹²F. Besenbacher and J. K. Nørskov, *Prog. Surf. Sci.* **44**, 5 (1993).
- ¹³T. Zambelli, J. Trost, J. Wintterlin, and G. Ertl, *Phys. Rev. Lett.* **76**, 795 (1996).
- ¹⁴J. Wintterlin, J. Trost, S. Renisch, R. Schuster, T. Zambelli, and G. Ertl, *Surf. Sci.* **394**, 159 (1997).
- ¹⁵(a) Y. Zeiri, J. J. Low, and A. Goddard III, *J. Chem. Phys.* **84**, 2408 (1986); (b) Y. Zeiri, *Surf. Sci.* **231**, 408 (1990).
- ¹⁶J. D. Beckerle, A. D. Johnson, and S. T. Ceyer, *Phys. Rev. Lett.* **62**, 685 (1989).
- ¹⁷G. Szulczewski and R. J. Levis, *J. Chem. Phys.* **103**, 10238 (1995).
- ¹⁸C. Åkerlund, I. Zoric, B. Kasemo, A. Cupolillo, F. Bautier de Mongeot, and M. Rocca, *Chem. Phys. Lett.* **270**, 157 (1997).
- ¹⁹B. Kulginov, M. Persson, and C. Rettner, *J. Chem. Phys.* **106**, 3370 (1997).
- ²⁰L. Romm, Y. Zeiri, and M. Asscher, *J. Chem. Phys.* **108**, 8605 (1998).
- ²¹J. D. Beckerle, A. D. Johnson, and S. T. Ceyer, *J. Chem. Phys.* **93**, 4047 (1990).
- ²²C. Åkerlund, I. Zoric, and B. Kasemo, *J. Chem. Phys.* **109**, 737 (1998).
- ²³L. Romm, Y. Zeiri, and M. Asscher, *J. Chem. Phys.* **110**, 3153 (1999).
- ²⁴(a) R. R. Lucchese and J. C. Tully, *J. Chem. Phys.* **81**, 6313 (1984); (b) A. C. Kummel, G. O. Sitz, R. N. Zare, and J. Tully, *ibid.* **89**, 6947 (1988).